# LIFECYCLE COST ASSESSMENT OF HIGH STRENGTH CARBON AND STAINLESS STEEL GIRDER BRIDGES

**Burak KARABULUT[a,*], Gonçalo FERRAZ[a], and Barbara ROSSI[a,b]**

[a] Department of Civil Engineering, KU Leuven, Belgium

Jan Pieter de Nayerlaan 5, Sint-Katelijne-Waver, Belgium.

Email: burak.karabulut@kuleuven.be

[b] University of Oxford, Department of Engineering Science, Oxford, UK

Email: barbara.rossi@new.ox.ac.uk

**Keywords**: Bridge design; Comparative lifecycle cost assessment (LCCA); Fatigue verification; Duplex stainless steel; Hot spot stress method.

**Abstract**. *This paper addresses the lifecycle cost assessment of a steel girder bridge considering the material costs and maintenance activities along the bridge's lifecycle. A reference highway bridge case study is chosen. It was initially designed using carbon steel S355. Two more steel grades are included in the comparison: high strength carbon steel S460 and duplex stainless steel EN 1.4162. For each design option, fatigue appears to be the driving design criterion for the following critical welded details: transversal stiffeners, cope holes and full penetration butt welds in the flanges. In addition to ultimate limit state verifications, specific attention is therefore given to fatigue through the use of different verification methods: the well-known nominal stress method and the hot spot stress method. It is concluded that the net present value of the lifecycle cost of the stainless steel option is attractive compared to painted the carbon steel options.*

## 1 STATE OF THE ART

### 1.1 General positioning of the problem

The use stainless steel is increasing in several sectors including the construction sector, due to the combination of high strength, aesthetical appearance, corrosion resistance leading to durability and low maintenance. When considering stainless steel, four different families may be distinguished based on their respective microstructures: martensitic, ferritic, austenitic

and duplex (an austenitic-ferritic microstructure) and, in recent years, duplex grades have gained popularity in (civil) structures requiring high strength and corrosion resistance, such as highway bridges, offshore platforms and nuclear power plants. This is also thanks to their good fatigue resistance (Branco et al., 2001; Zilli et al., 2008). The duplex grades EN 1.4062 and EN 1.4162, included in (EN 10088-2, 2014; EN 1993-1-4 A1, 2015) as well as in the Design Manual for Structural Stainless Steel (DMSSS, 2017), are characterized by a lower Nickel and increased Nitrogen contents, resulting in a significant cost reduction (as well as stability) when compared to more traditional austenitic equivalents (EN 1.4404) or more conventional duplex grades such as EN 1.4462. Furthermore, numerous studies (Iversen, 2006; Merello et al., 2003; Olsson and Snis, 2007; Wei et al., 2008) have demonstrated superior mechanical properties of duplex grades when compared to austenitic grades (see Fig. 1) and equal or better corrosion resistance. In addition, duplex grades are today welded with standard welding processes as for conventional mild steel grades (Baddoo, 2008; Fortan et al., 2020; Karabulut et al., 2020). All these progresses explain why these grades are more and more used in welded structures in corrosive environment, such as bridges in coastal areas.

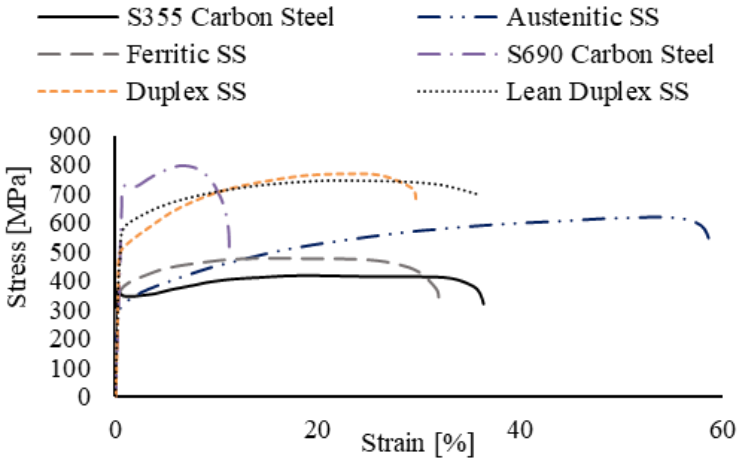


**Fig. 1.** Stress-strain curves for different steel grades.

Today, European codes and design books include fatigue design rules for steel and composite structures (EN 1993-1-9, 2005; EN 1993-2, 2006; Hobbacher, 2016; Nussbaumer et al., 2011). In the most recent draft revision of (EN 1993-1-9, 2005), it is stated that fatigue design rules apply to carbon steel, stainless steel and unprotected weathering steels if they comply with the toughness recommendations given in (EN 1993-1-10, 2005). In (DMSSS, 2017; EN 1993-1-4, 2006), duplex is said to be characterized by sufficient impact energy down to temperatures of -40 °C and (EN 1993-1-9, 2005) is recommended for fatigue design of these grades.

As highlighted in the background documentation of Eurocode fatigue design rules (Brozzetti et al., 2018), the fatigue strength curves (SN-curves) are mostly derived from experiments on carbon steel uncoated details with nominal yield strength ranging between 235 and 400 MPa. It is widely accepted that fatigue failure in welded components is due to welding-related imperfections (such as residual stresses, geometrical misalignment, mismatch, lack of penetration, weld convexity, etc.)

leading to concentration of stresses and so it is currently not possible to exploit higher base material strengths in the design against fatigue. Several studies however show that the proposed detail categories tend to be conservative for details made of higher strength steels (Branco et al., 2001; Habraken et al., 2019; Karabulut et al., 2020; Liljas and Ericsson, 2002; Zilli et al., 2008). In this paper, higher strength steels are considered, and their fatigue behaviour carefully taken into account. A highway girder bridge is investigated where the main girders are made of duplex stainless steel instead of mild carbon steel (S355 or S460). In addition to the static design aspects at ultimate limit states (ULS) and serviceability limit states (SLS), fatigue design of three fatigue-prone details is addressed following the nominal stress method (NSM) and the hot spot stress method (HSSM), where the hot spot (HS) stress is calculated using the finite element method (FEM). All bridges (made of different steel) are compared and their lifecycle cost are calculated taking into account maintenance activities.

### 1.2 Fatigue verification techniques

The most popular methods used in fatigue design of critical welded details present in bridges are the stress life methods: the nominal stress method (NSM), hot spot stress method (HSSM), the notch stress approach (NSA) and fracture mechanics (Ye et al., 2014). The NSM is the most commonly adopted one as it uses the straightforward SN-curve approach where a linear or multilinear relationship is defined between the applied stress range and the detail's fatigue life. Yet, when complex multi-dimensional loading conditions or complex geometries whose fatigue capacity cannot be represented by a simple detail category exist, the NSM cannot be used. In that case, one needs to seek for local stress approaches such as the HSSM (Aygül et al., 2012; Poutiainen et al., 2004; Xiao and Yamada, 2004).

The HS stress is defined as magnified nominal stress with a stress concentration factor (SCF). This factor is calculated based on either linear or quadratic extrapolation of surface stresses to the weld toe, where the fatigue cracks initiate. Currently the method is addressed in the Eurocodes (EN 1993-1-9, 2005), however the detailed guidance is available in the International Institute of Welding (IIW) guidelines (Hobbacher, 2016). The HS stress can be evaluated either experimentally or numerically. In the case of fatigue design of steel bridges, the finite element method (FEM) is usually preferred, because it is the least time-consuming method. However, in case of numerical computation of the HS stress, the evaluated value is highly dependent on the model topology as well as FEM parameters. Therefore, many studies in the literature investigated the sensitivity of HS stress to these parameters, leading to improvement of the modelling rules and new guidelines (Aygül et al., 2012; Doerk et al., 2003; Fricke et al., 2017, 2002; Ji et al., 2013; Karabulut et al., 2020, 2018; Lee et al., 2010; Liu et al., 2014; Morgan and Lee, 1997; Niemi et al., 2018, 2006; Park and Kim, 2014).

### 1.3 Fatigue behaviour of duplex welded components

The S-N curves of stainless steel details which are included in the background documents of the Eurocodes or in the scientific papers are usually derived for specimens made of austenitic or conventional duplex grades (Branco et al., 2001; Ericsson et al., 2003; Liljas and Ericsson, 2002; Zilli et al., 2008). The knowledge on the fatigue behaviour of lean duplex welded components is today quite scarce, as the existing research on these grades is mostly limited to the material or microstructural level where toughness, hardness, roughness or the effects of post weld treatment (PWT) on the microstructure are mostly investigated (Ericsson et al., 2003; Liljas and Ericsson, 2002; Peng et al., 2019). The fatigue behaviour of welded details made of duplex EN 1.4462 was however investigated in the European Commission (EC) project "BRIDGEPLEX" (Zilli et al., 2008), and some of the detail categories in (EN 1993-1-9, 2005) were shown to be significantly conservative for these details. Similar observations were published by (Branco et al., 2001) in which the same grade, especially used in welded transversal stiffeners, turn out to have much higher fatigue resistance than the proposed detail category in the Eurocode (EN 1993-1-9, 2005). However, this was attributed to the fact that these welds were deposited by the Tungsten Inert Gas (TIG) welding process, and therefore weld concavity led to reduced stress concentration factor (SCF) and thus higher fatigue lives.

The existing limited research data on the fatigue behaviour of the duplex EN 1.4162 grade at the structural level show that it has similar fatigue strength to that of higher strength steel (HSS) or more conventional duplex grades (Karabulut et al., 2020; Liljas and Ericsson, 2002). It was also concluded that the Eurocode detail categories are conservative, yet safely applicable when a fixed slope of m = 3 is considered (Karabulut et al., 2020).

### 1.4 Weight reduction and lifecycle cost assessment

There is today a demand for the optimization of civil structures, so that more economic, lighter, efficient and environmentally friendly structures are built. Fabrication of customized complex cross-sections, such as those present in bridges, often uses welding. The EC project "BRIDGEPLEX" (Zilli et al., 2008) puts emphasis on the economic gain that can be achieved in an orthotropic deck bridge when carbon steel details are replaced by high strength duplex stainless steel ones. The beneficial effect of higher strength steel grade was combined with low maintenance costs, and the duplex option turns out to have a lower lifecycle cost (LCC). Very similar observations were made in (Habraken et al., 2019; Lemma et al., 2020; Pedro et al., 2018, 2017) where the possible weight reduction when S690 is used instead of S355 in a steel girder bridge is calculated. The weight reduction of structures via the use of higher strength materials is reported in many other studies (Budano et al., 2007; Günther, 2005; Lagerqvist et al., 2007; Sedlacek et al., 2002; Shi et al., 2014) but, to the authors' best knowledge, most of these studies did not consider fabrication/maintenance costs.

## 2 CASE STUDY

### 2.1 Introduction

The ultimate goal of this chapter is to assess the weight reduction in a girder bridge when higher strength steel grades are employed instead of the more traditional S355 carbon steel. The higher strength steels considered in this study are the S460 structural carbon steel grade according to (EN 10025-3, 2019) and the duplex stainless steel EN 1.4162 according to (EN 10088-2, 2014). The case study proposed by (Pedro et al., 2018, 2017) is presently chosen as the reference bridge. In the current paper, the bridge is assumed to be located in a coastal area in Belgium where the needed Corrosion Resistance Class (CRC) is considered to be 3 with the following points taken into account according to (DMSSS, 2017; EN 1993-1-4 A1, 2015):

- The measured distance from the sea M is between 0.25 km and 1 km, whereas the distance from the roads exposed to de-icing salts S is smaller than 0.01 km. Therefore, the risk of exposure to chlorides from salt, water or de-icing salts F1 is -7.
- A gas chromatograph measures the average sulphur dioxide concentration below 10 $\mu g/m^3$ thus resulting in low risk of exposure to sulphur dioxide, and F2 is taken as 0. No specified cleaning regime is envisaged.

The reference design (Habraken et al., 2019; Pedro et al., 2018, 2017) compares two design options made of S355 and S690. The comparative design studies the midspan of a highway girder bridge (80 m) with 5 spans with a total length of 360 m (Span CD in Fig. 2b). The ultimate objective of their study is to lose weight by reducing the cross-sectional areas, thus achieving better environmental performance (reduced maintenance areas, less welding volume, less labour cost). The weight reduction is 25 % in case the main girders are made of S690 instead of S355, and the lifecycle cost (LCC) is 2.2 % cheaper. However, due to reduced cross-sectional areas, the design option using S690 becomes very susceptible to local buckling as well as fatigue. Therefore, the authors proposed an alternative design solution, again with S690, but this time using additional longitudinal stiffeners on the girder webs as well as post-weld treatments (PWT) to improve the fatigue performance. In this case, the weight reduction reaches 32 % and the LCC becomes 3.2 % cheaper.

The current study elaborates on the designs of the 80 m long internal span (Span CD in Fig. 2b) where the combination of shear and bending moment is the most detrimental. The designs were performed based on the internal forces obtained from a finite framed element model of the bridge. The span configuration and the superstructure cross-section considered in the analysis can be seen in Fig. 2 and Fig. 3. The throat thicknesses of the welds shown in Table 1 are calculated according to (EN 1993-1-8, 2005) considering the resulting internal forces under the worst-case combination for ULS. In each of the

design options, the bridge deck is made of C35/45 grade concrete, substructure elements such as the piers and the abutments are made of C30/37 grade concrete.

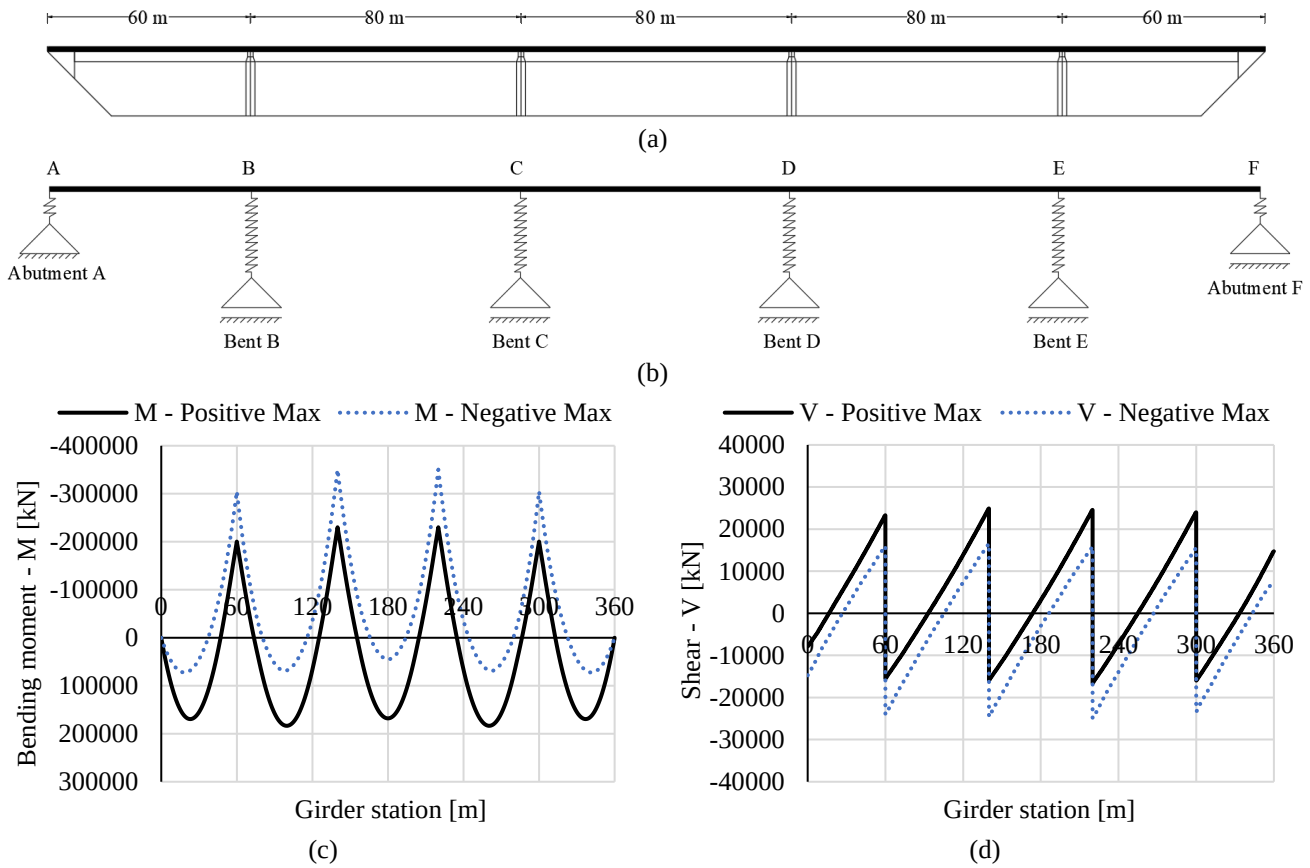


**Fig. 2.** Span configuration: (a) bridge spans (Pedro et al. 2017); (b) analysis model; (c) bending moment distribution along the bridge superstructure; (d) shear force distribution along the bridge superstructure.

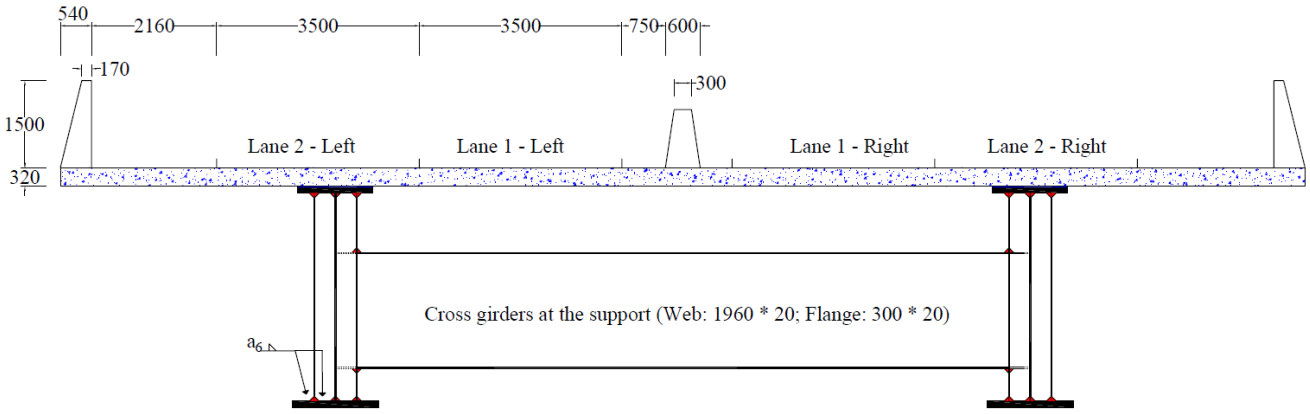


(a)

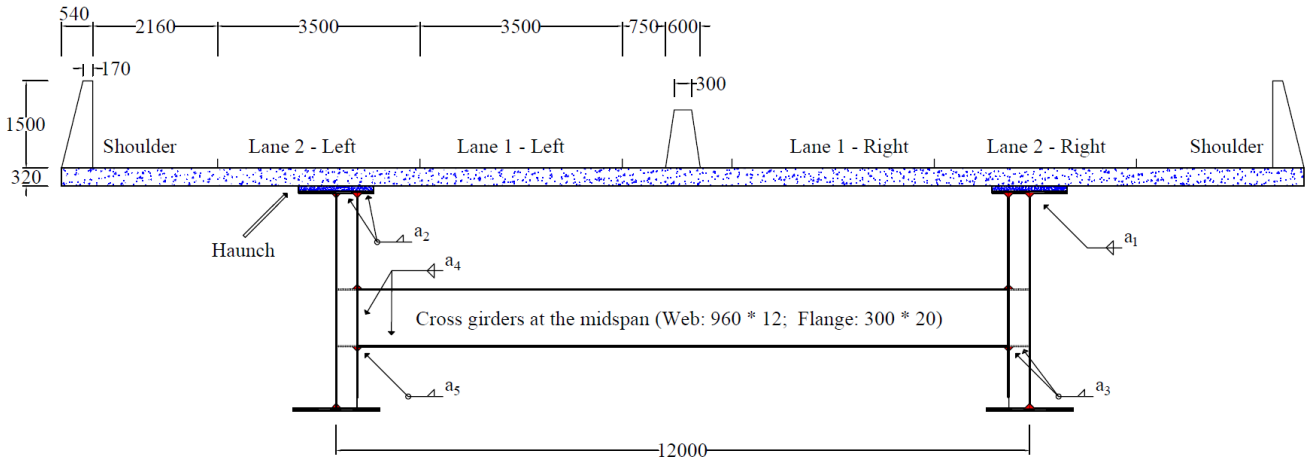


(b)

**Fig. 3.** Analysis model of the bridge superstructure cross-section: (a) at the support; (b) at the midspan (units in mm).

**Table 1.** Overview of weld throat thicknesses.

| Weld throat thicknesses – a | $a_1$ [mm] | $a_2$ [mm] | $a_3$ [mm] | $a_4$ [mm] | $a_5$ [mm] | $a_6$ [mm] |
|---|---|---|---|---|---|---|
| S355 | 10 | 10 | 10 | 10 | 10 | 10 |
| EN 1.4162 | 8 | 10 | 8 | 6 | 10 | 10 |
| S460 | 9 | 10 | 8 | 6 | 10 | 10 |

### 2.2 Design loads

The factored load and combinations were set according to (EN 1990, 2002) taking into account the requirement of the Belgian national annexes (EN 1990 ANB, 2012). The following loads were included:

- Self-weight of the steel and concrete components with density of 77 kN/m$^2$ and 25 kN/m$^2$ respectively.
- 5.1 kN/m is applied as uniformly distributed line load per safeguarding barrier.
- 1.71 kN/m is applied as uniformly distributed line load per main girder representing the haunches.

- 0.72 kN/m$^2$ is applied as uniformly distributed surface load representing the permanent form loads.
- 0.30 kN/m$^2$ is applied as uniformly distributed surface load representing pouring of the concrete (the finishing layer).
- 1.44 kN/m$^2$ is applied as uniformly distributed surface load representing wearing surface (top layer of a sealed road).
- A temperature variation from +15 °C to -18 °C is considered.
- Wind loads are considered according to (EN 1991-1-4, 2005) and Belgian national Annex (EN 1991-1-4 ANB, 2010).
- Load model 1 as defined in (EN 1991-2, 2003) considering the Belgian national Annex (EN 1991-2 ANB, 2011) is applied for the verifications at the ultimate limit state (ULS).
- Fatigue load model 3 (FLM3) as defined in (EN 1991-2, 2003) is used for verifications at the fatigue limit state (FLS).
- Creep and Shrinkage effects are considered in the material model of concrete following the information given in (Habraken et al., 2019; Pedro et al., 2018, 2017) where single stage casting is considered.

**2.2 Cross-section resistance checks of the main girders**

The nominal mechanical strength of the carbon steel grades is provided in (EN 10025-3, 2019), whereas the properties of stainless steel grades are provided in the most recent design guidelines for structural stainless steel (DMSSS, 2017; EN 10088-2, 2014; EN 1993-1-4, 2006; EN 1993-1-4 A1, 2015). Verifications for the ULS are performed following (EN 1993-1-1, 2005; EN 1993-1-4, 2006; EN 1993-1-5, 2006) for the cross-sectional resistance checks as well as instability checks such as lateral-torsional buckling (LTB) and shear buckling (SB). Composite action between the concrete deck and the steel main girders is considered according to (EN 1994-1-1, 2004; EN 1994-2, 2005). Checks for SLS are carried out for the midspan deformation of the studied main girders according to (EN 1990, 2002; EN 1993-2, 2006). The deformation at midspan is analysed under the live load case of load model 1. The maximum deflection $\delta(\psi_1 Q_{k1})$ at midspan should not exceed L/500 where L is the span length. Some of the important differences in the design parameters between the carbon and stainless steel options are summarized in Table 2. These parameters are: E – the Young's modulus of the material, $\rho$ – the density of the material, $\varepsilon$ – the non-dimensional coefficient for cross-section classification, $\gamma_m$ – the safety factors, $\bar{\lambda}_{LT,0}$ – the non-dimensionless limiting slenderness for LTB, and the effective stiffener cross-section according to Chapter 9 of (EN 1993-1-5, 2006). In the designs, the thickness effect on the mechanical strength is considered according to (EN 10025-3, 2019; EN 10088-2, 2014) for carbon steel and stainless steel design options. It is important to note that there is currently no information available in the norms for stainless steels that are thicker than 75 mm.

The same type of cross-girders is employed for each design option, the dimensions of which is given in Fig. 3. Cross girders are connected to the T-stiffeners of the web at a distance of each 8 meters. As given in (Habraken et al., 2019; Pedro et al., 2018, 2017), for the S355 bridge, T-stiffeners were used every 8 m through the entire span. Besides, flat stiffeners

every 2 m are considered over a portion of 24 m from the supports and then spacing increases to 4 m for the rest of the span. More information about the detailing of that design can be found in the reference case, Annex 7 of (Habraken et al., 2019). All these verifications are presented in Fig. 5. for the given cross-sections in Fig. 4. In Fig. 5, $M_{Ed}$ refers to the design value of maximum bending moment, $M_{c,Rd}$ is the cross-sectional bending moment resistance, $M_{b,Rd}$ is the moment resistance of the cross-section considering instability (lateral torsional buckling for the current case), $V_{Ed}$ is the design value of the maximum shear force and $V_{bw,Rd}$ is the shear resistance of the cross-section considering instability (shear bucking for the current case).

The designs of the bridges made of EN 1.4162 and S460 use T-stiffeners for a greater stability against shear buckling. The positioning of the stiffeners is the same as in the reference design. Those stiffeners are designed according to (EN 1993-1-5, 2006) considering also Chapter 5.7 of (EN 1993-1-4, 2006) and Chapter 6.4.5 of (DMSSS, 2017) for stainless steel.

**Table 2.** Differences in design parameters.

| Design options | $f_y$ [MPa] | E [GPa] | ρ [kg/m$^3$] | ε | $\gamma_{m0}$ | $\gamma_{m1}$ | $\gamma_{m2}$ | $\bar{\lambda}_{LT,0}$ | Effective stiffener cross-section |
|---|---|---|---|---|---|---|---|---|---|
| S355 | 355 | 210 | 7850 | 0.81 | 1.0 | 1.0 | 1.25 | 0.2 | 15 $\varepsilon t_w$ |
| EN 1.4162 | 450 | 200 | 7700 | 0.71 | 1.1 | 1.1 | 1.25 | 0.4 | 11 $\varepsilon t_w$ |
| S460 | 460 | 210 | 7850 | 0.71 | 1.0 | 1.0 | 1.25 | 0.2 | 15 $\varepsilon t_w$ |

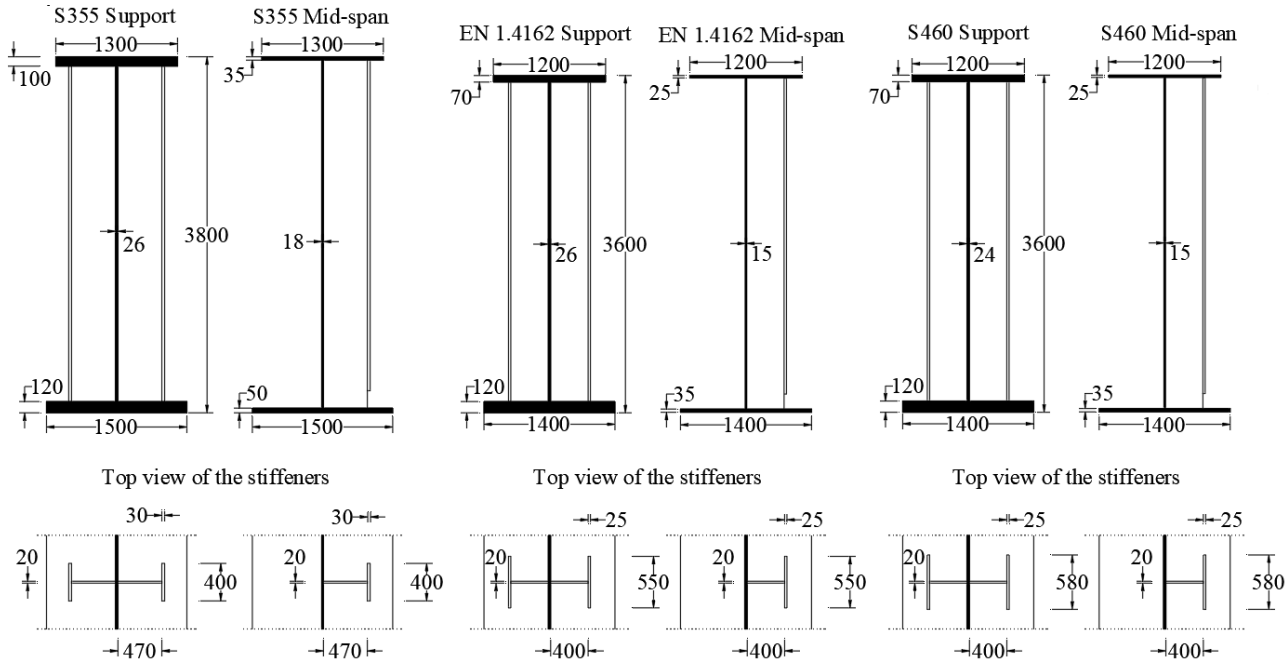


**Fig. 4.** Design of the main bridge girders: cross-section geometries made of EN 1.4162 versus S355 and S460.

It is worth noting that the same limiting ratios as those provided by (Pedro et al., 2018, 2017) for S355 are obtained at the support and midspan as shown in Fig. 5, suggesting that this analysis is validated.

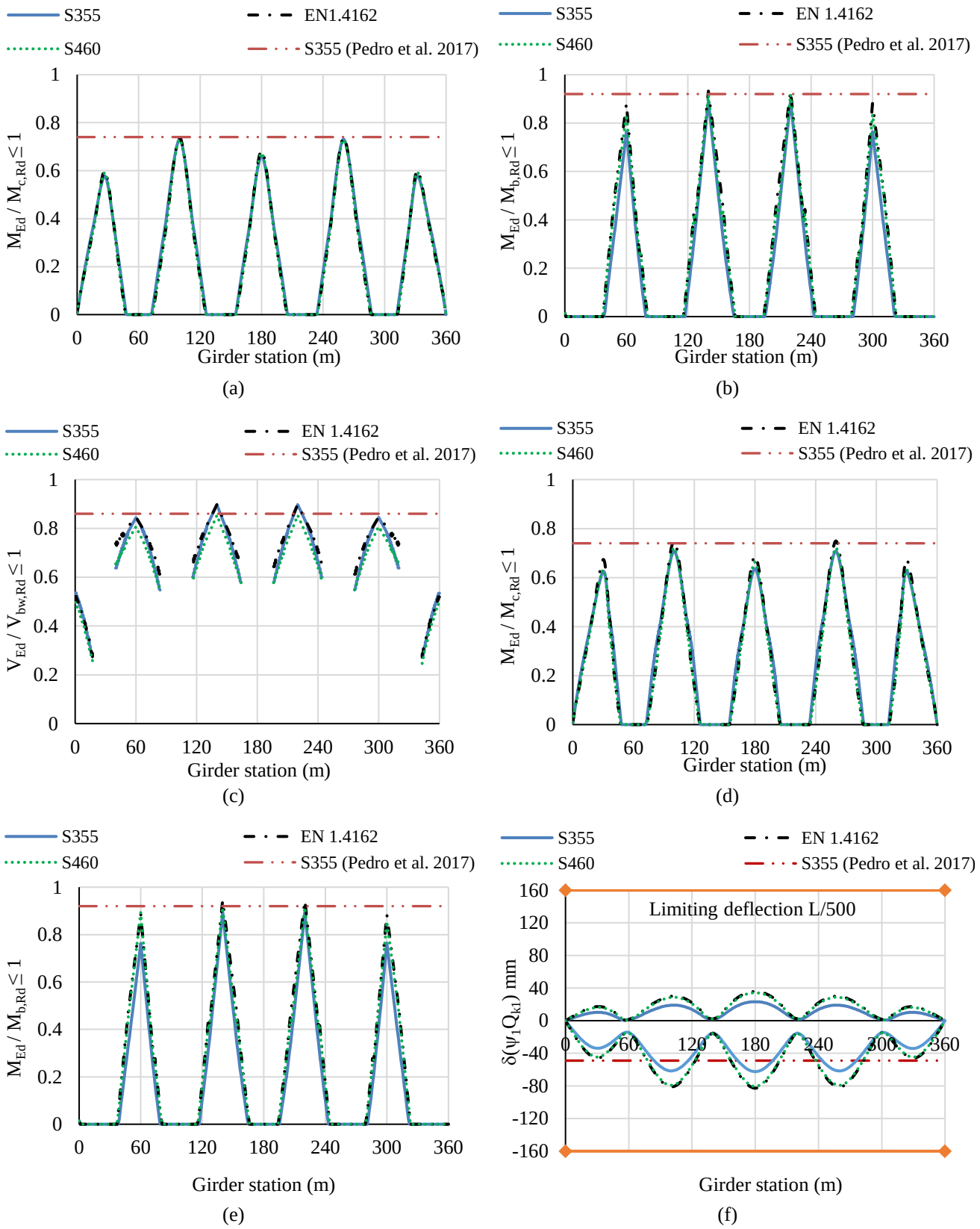


**Fig. 5.** Design checks: (a) bending resistance – positive flexure; (b) LTB – negative flexure; (c) shear buckling; (d) positive flexure - shear interaction; (e) negative flexure – shear interaction; (f) SLS checks for deflection.

## 3 FATIGUE DESIGN OF THE DETAILS

Fatigue is often one of the governing design criteria for a continuous highway girder bridge because of the presence of a series of critical welded details. Since welding leads to imperfections such as geometrical discontinuities inducing stress concentrations, residual stresses as well as defects in the form of inclusions or mismatch, the welded spots are more susceptible to fatigue crack initiation and propagation, followed by fatigue failure. In cases where high strength steels are employed, the designers put their utmost attention on weight reduction possibilities resulting in increased proneness to fatigue because of reduced plate thicknesses and increased fluctuating stress ranges.

In this chapter, the fatigue verifications of the selected critical welded details are carried out according to the NSM following (EN 1993-1-9, 2005; EN 1993-2, 2006) and then based on the HSSM by means of finite element (FE) analysis.

### 3.1 Selection of fatigue-prone details

Several studies compiling real fatigue damages in bridges have been studied during the last decades (ASCE, 1982; Duga et al., 1983; Reed et al., 1983). And, more recently, numerous observations concentrating on a series of fatigue prone details in bridges have been published by (Al-Emrani and Kliger, 2009; Haghani et al., 2012; Kubiš and Ryjáček, 2017). Those papers have led to the European Convention for Constructional Steelwork (ECCS) publishing a compilation of all these observations and a chart of 12 most common fatigue susceptible details in bridges (Lukic and Kühn, 2020). Based on this chart, we can conclude that 75 to 80 % of these details are welded ones. In the current paper, 8 of these critical welded details for bridges applications are present in the bridge. A scheme of these details can be seen in Fig. 6, with the detail categories of (EN 1993-1-9, 2005), as listed below:

- (a) Cover plate attached to the bottom flange of the longitudinal main bridge girder with the welds all around submitted to tension;
- (b) Longitudinal fillet welds attaching the web and the flanges;
- (c) Shear studs for composite action between the steel girders and concrete bridge deck;
- (d) Transversal stiffeners with the welds transverse to the loading direction;
- (e) Transversal stiffeners with the welds longitudinal to the loading direction;
- (f) Tapered flanges inducing additional stress concentration;
- (g) Cope holes on the main bridge girders;
- (h) Full penetration butt welded joints in flanges.

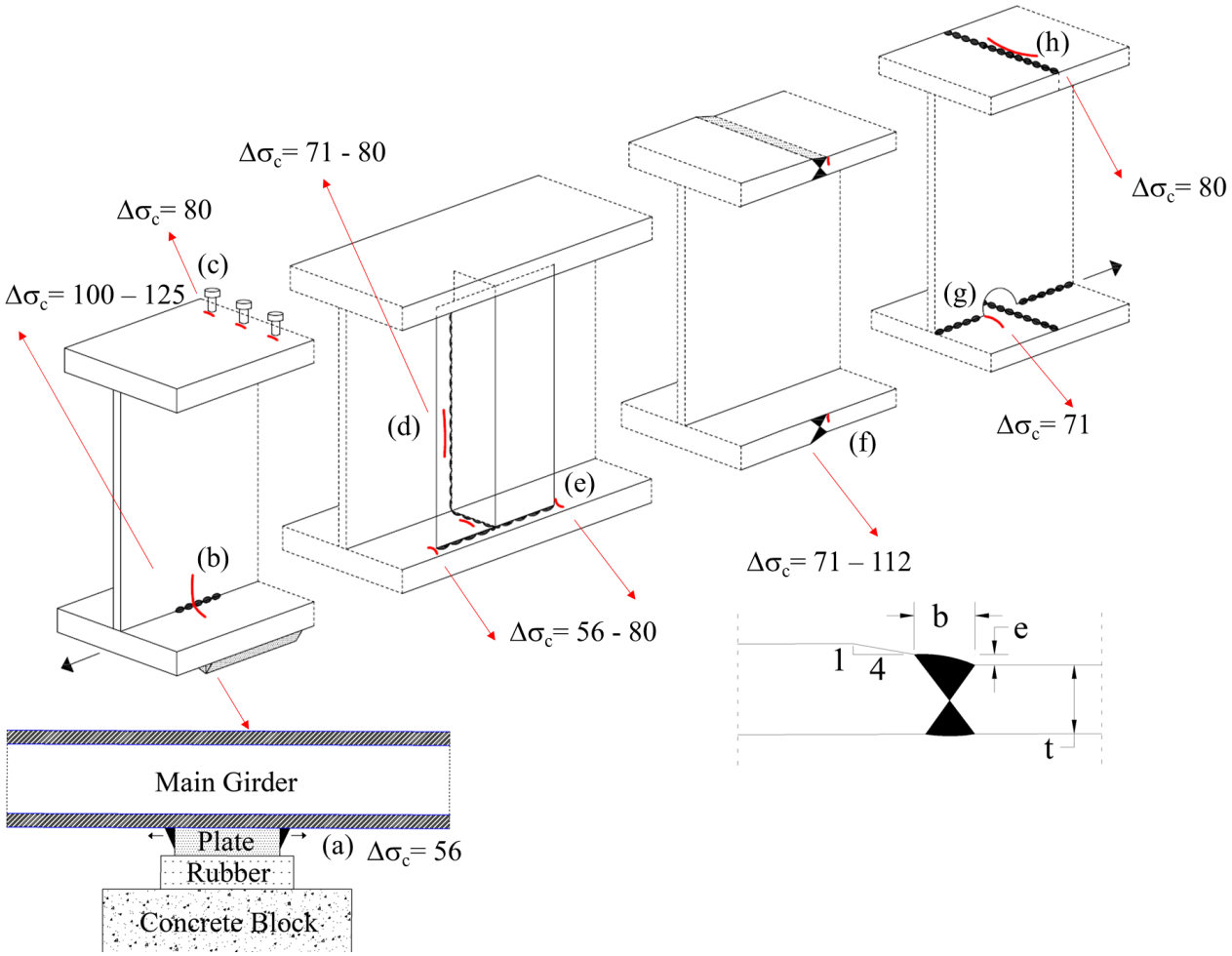


**Fig. 6.** Overview of the critical fatigue details in the studied bridge girder.

### 3.2 Fatigue verifications with the nominal stress method

The NSM is commonly adopted in Europe to design bridges against fatigue, due to its efficiency. It is based on a nominal (global) stress range computed in the considered detail which is combined with the corresponding SN-curve where the stress magnifying effects (of for example a weld) are included. The minimum and maximum stress are determined far from the stress concentration zone where the stress field is homogenous and can be computed using the traditional theories of structural mechanics for linear elastic material.

For the chosen bridge, the stress ranges acting in each considered detail are obtained under the application of fatigue load model 3 (FLM3) according to (EN 1991-2, 2003). FLM3 is represented by a maximum truck axle load of 480 kN acting on 4 axles (the load is distributed on a patch of 0.4 m by 0.4 m representing the wheel contact surface area). In accordance with the national annex, a second truck with a total axle load of 120 kN has also been modelled, following the first truck at a distance of 40 m. The equivalent stress range is calculated following Equations (1)-(6) using the damage equivalent factors for the safe life method according to (EN 1993-1-9, 2005).

$$\lambda = \lambda_1 . \lambda_2 . \lambda_3 . \lambda_4 < \lambda_{max} \quad (1)$$

$$\lambda_2 = \frac{Q_{m1}}{Q_0} \left(\frac{N_{Obs}}{N_0}\right)^{\frac{1}{5}};\ Q_0 = 480\ kN;\ N_0 = 0.5\ 10^6 \quad (2)$$

$$Q_{m1} = \left(\frac{\sum n_i {Q_i}^5}{\sum n_i}\right)^{1/5} \quad (3)$$

$$\lambda_3 = \left(\frac{t_{Ld}}{100}\right)^{1/5} \quad (4)$$

$$\Delta\sigma_E = \lambda \left|\sigma_{Qmax} - \sigma_{Qmin}\right| \quad (5)$$

$$\gamma_{Ff} . \gamma_{Mf} . \Delta\sigma_E \leq \Delta\sigma_C \quad (6)$$

where $\lambda$ is the damage equivalent factor according to (EN 1993-1-9, 2005), $\lambda_1$ and $\lambda_{max}$ are the factors based on the span length and moments for road bridges specified in Fig. 7, $\lambda_2$ factor depends on the traffic volume specified by $Q_{m1}$ which is the mean gross weight of the lorries in the slow lane in kN, $N_{Obs}$ is the overall number of lorries per year in the slow lane, $Q_i$ is the gross weight of the $i^{th}$ lorry in the slow lane in kN, $n_i$ is the number of lorries, $\lambda_3$ factor depends on the design life of the bridge which is $t_{Ld}$, $\lambda_4$ factor depends on traffic on other lanes, $\Delta\sigma_E$ is the equivalent stress range, $\sigma_{Qmax}$ and $\sigma_{Qmin}$ are the maximum and minimum calculated stress ranges for the critical detail under the applied fatigue load model, $\gamma_{Ff}$ and $\gamma_{Mf}$ are partial factors for equivalent constant amplitude stress range and fatigue strength respectively and $\Delta\sigma_C$ is the nominal stress of the detail category. Maximum and minimum calculated stress ranges shown in Fig. 9 are determined according to the influence line analysis, the results of which are given in Fig. 8 for the EN 1.4162 design option.

The following conditions were considered while calculating the damage equivalent factors and equivalent stress ranges:

- $N_{Obs}$ is taken as $0.5\ 10^6$ according to (EN 1991-2, 2003);
- $Q_{m1}$ is taken as 445 kN according to (Nussbaumer et al., 2011);
- $t_{Ld}$ is taken as 100 years;
- $\gamma_{Ff} = 1.0$ and $\gamma_{Mf} = 1.35$ according to (EN 1993-1-9, 2005) for high consequence of failure with the safe life approach.

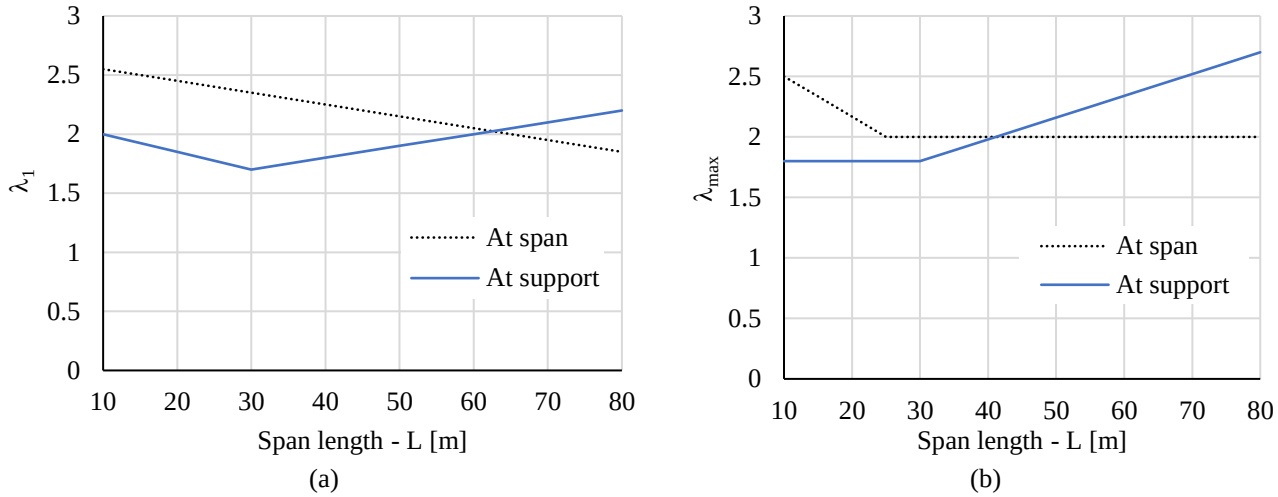


**Fig. 7.** Damage equivalent factors: (a) $\lambda_1$; (b) $\lambda_{max}$.

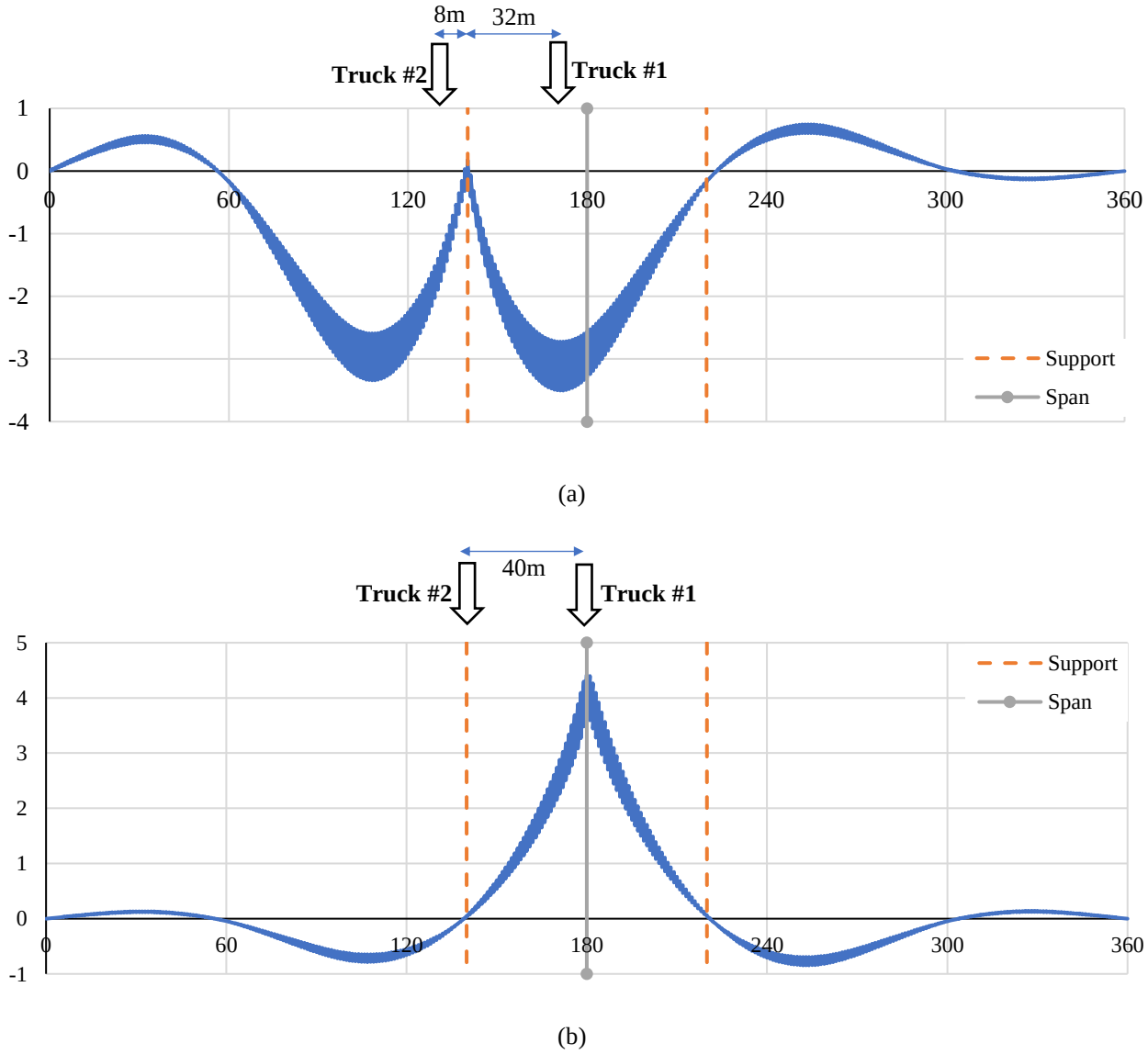


**Fig. 8.** Influence line analysis for span CD: (a) Influence line for the support with trucks positioned at maximum negative flexure; (b) Influence line for the midspan with trucks positioned at maximum positive flexure.

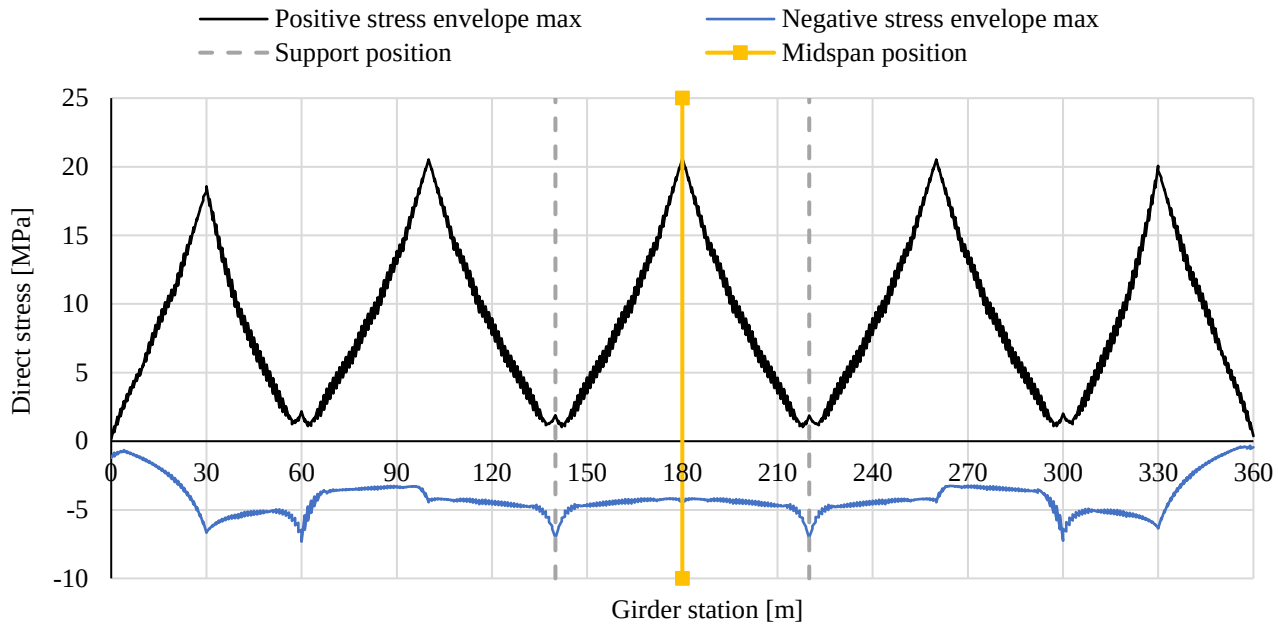


(a)

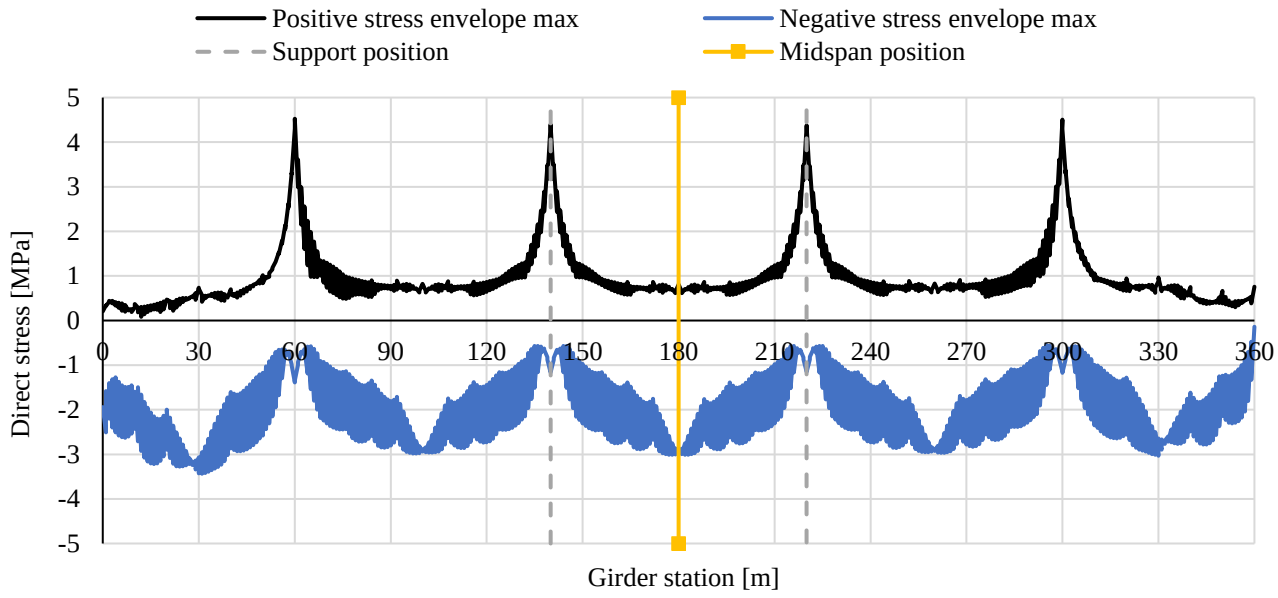


(b)

**Fig. 9.** Fluctuating stress ranges as the live load FLM3 moves on the main girders for design option EN 1.4162: (a) bottom flange; (b) top flange.

As can be seen in Table 3, the most critical 3 fatigue details could be categorized as transversal stiffeners, full penetration butt welds of the flanges and cope holes. These details are considered as the most critical ones because they have the highest applied load versus resistance ratios. The critical locations of each of these details appear to be at the bottom flange at midspan. These details turn out to be more critical for higher strength design options because of the greater mechanical strength of the material which allows smaller thicknesses at midspan resulting in higher stress ranges as well.

**Table 3.** Fatigue design of all selected details according to the nominal stress method.

| Detail | $\Delta\sigma_c$ [MPa] | Size effect – $k_s$ | $\frac{\gamma_{Ff}\cdot\gamma_{Mf}\cdot\Delta\sigma_{E2}}{\Delta\sigma_c}$ | | | Location |
|---|---|---|---|---|---|---|
| | | | S355 | EN 1.4162 | S460 | |
| (a) | 56 | - | 0.52 | 0.58 | 0.59 | Bottom flange at support |
| (b) | 100 | - | 0.48 | 0.68 | 0.68 | Bottom flange at midspan |
| (c) | 80 | - | 0.23 | 0.25 | 0.26 | Bottom flange at support |
| (d) | 80 | - | 0.60 | 0.85 | 0.85 | Bottom flange at midspan |
| (e) | 56 | - | 0.52 | 0.58 | 0.59 | Bottom flange at support |
| (f) | 112 | 1 | 0.09 | 0.09 | 0.09 | Top flange at midspan |
| (f) | 112 | 0.94 | 0.50 | 0.65 | 0.65 | Bottom flange at midspan |
| (f) | 112 | 0.81 | 0.22 | 0.22 | 0.23 | Top flange at support |
| (f) | 112 | 0.73 | 0.36 | 0.40 | 0.40 | Bottom flange at support |
| (g) | 71 | - | 0.68 | 0.95 | 0.96 | Bottom flange at midspan |
| (h) | 80 | 1 | 0.13 | 0.13 | 0.13 | Top flange at midspan |
| (h) | 80 | 0.94 | 0.69 | 0.90 | 0.91 | Bottom flange at midspan |
| (h) | 80 | 0.81 | 0.31 | 0.31 | 0.32 | Top flange at support |
| (h) | 80 | 0.73 | 0.50 | 0.56 | 0.57 | Bottom flange at support |

Both the full penetration butt welds and the cope holes detail categories can be improved straightforwardly as follows:

- Full penetration butt welded joints can be upgraded from $\Delta\sigma_C$ = 80 MPa to $\Delta\sigma_C$ = 90 MPa by reducing the height of the weld convexity from 20% to 10 % and by making the welds flush ground;
- The cope holes can be upgraded from $\Delta\sigma_C$ = 71 MPa to $\Delta\sigma_C$ = 90 MPa by applying a full cross-section butt welds at the region where cope holes are located. This applies only on the condition that the welds are ground flush and welding is performed from both sides and checked by non-destructive testing.

When it comes to the transversal stiffeners, they are unfortunately considered to be unavoidable due to susceptibility to shear buckling phenomenon of slender web in welded girders. Regarding the experimental fatigue behaviour of duplex EN 1.4162 welded stiffeners, a similar trend of fatigue resistance for duplex and high strength steel equivalents was already reported in the literature (Karabulut et al., 2020), pointing out conservatism of the current design rules in the fatigue verification of higher strength (stainless) steel grades. However, the higher fatigue resistance of these grades is currently not

reflected in any fatigue design norm and therefore this paper uses the published recommendations in (EN 1993-1-9, 2005) for the fatigue verification of high strength steel welded details.

### 3.3 Fatigue verifications with the hot spot stress approach

The NSM has the obvious drawbacks where the geometry of more complex details, complex multi-dimensional loading conditions, or size effects need to be captured when computing the local stresses (Poutiainen et al., 2004; Xiao and Yamada, 2004). Therefore, local stress concepts, such as the HSSM has gained a rising interest (Aygül et al., 2012). Thorough guidance is provided in the ECCS recommendations and IIW guidelines (Hobbacher, 2016; Nussbaumer et al., 2011).

#### 3.3.1 Sensitivity analysis

When calculating the HS stress by means of FE analysis, the results are dependent on the model parameters (Lee et al., 2010). Therefore, a sensitivity analysis has been here conducted on the following parameters: mesh size, mesh topology, element type (8-noded linear solid elements vs. 20-noded quadratic solid elements), integration algorithm (full vs. reduced integration), length of the evaluated detail, extrapolation function (linear vs. quadratic extrapolation), modelling of the butt weld inside the cope hole, shell vs. solid elements, weld angle (varying between 30° and 60°), weld convexity (45° vs. convex and concave welds). For this analysis, the cope hole in the main girder webs (detail (g) in Fig. 6) was selected, as this detail has the most complex geometry and the evaluated HS stress is expected to be sensitive to the previously mentioned FEM parameters. The FE analysis was carried out using the Abaqus/Standard software. The web, flange and welds are modelled as in Fig. 10, where both plates' ends are subjected to a uniform stress state corresponding to the evaluated equivalent stress range. The boundary conditions (BCs) do not restrain Poisson's effects. The introduced cope hole has a diameter of 60 mm.

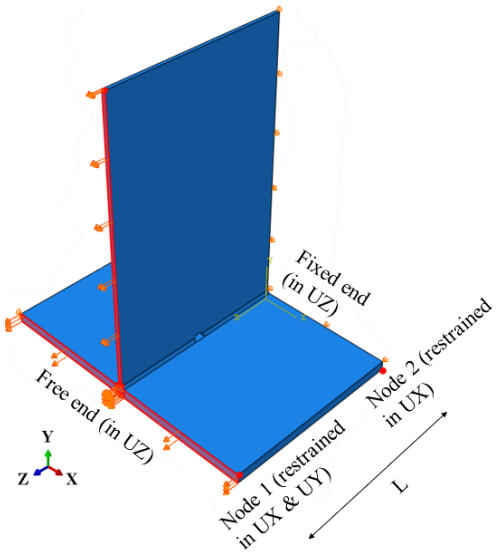


**Fig. 10.** FEM of the detail depicting the BCs and uniform force corresponding to the equivalent stress range.

An example of sensitivity analysis on the mesh size can be seen in Fig. 11 for the EN 1.4162 design option. Regarding the selected model parameters, such as the mesh size, the computational time and accuracy of FE results (convergence) are interconnected and therefore a compromise should be sought. For the fatigue design of welded details, the IIW guideline recommends using either fine or coarse meshes, i.e. mesh size relative to plate thickness ≤ 0.4 t and ≤ 1.0 t respectively. As can be seen in Fig. 11(a-c), three meshes from coarse to very fine were studied. The analysis was performed using 8-noded linear solid elements (C3D8R in the element library), using at least 4 elements through the thickness as suggested by (DNV-RPC203, 2011; Niemi et al., 2006). The computed HS stress along the flange can be seen in Fig. 11(d) with the linear extrapolation according to the IIW guideline given on the vertical axis. The maximum difference in the computed HS stress between the coarse and very fine mesh group seems to be 1.8% for HS1 and 0.41% for HS2 (see Fig. 12b for HS1 and HS2). It must be noted that HS2 results in greater SCFs, which is why it is more critical, and therefore Table 4 gives an overview of sensitivity analysis only for HS2. More details about the sensitivity analysis can be found in (Karabulut et al., 2018).

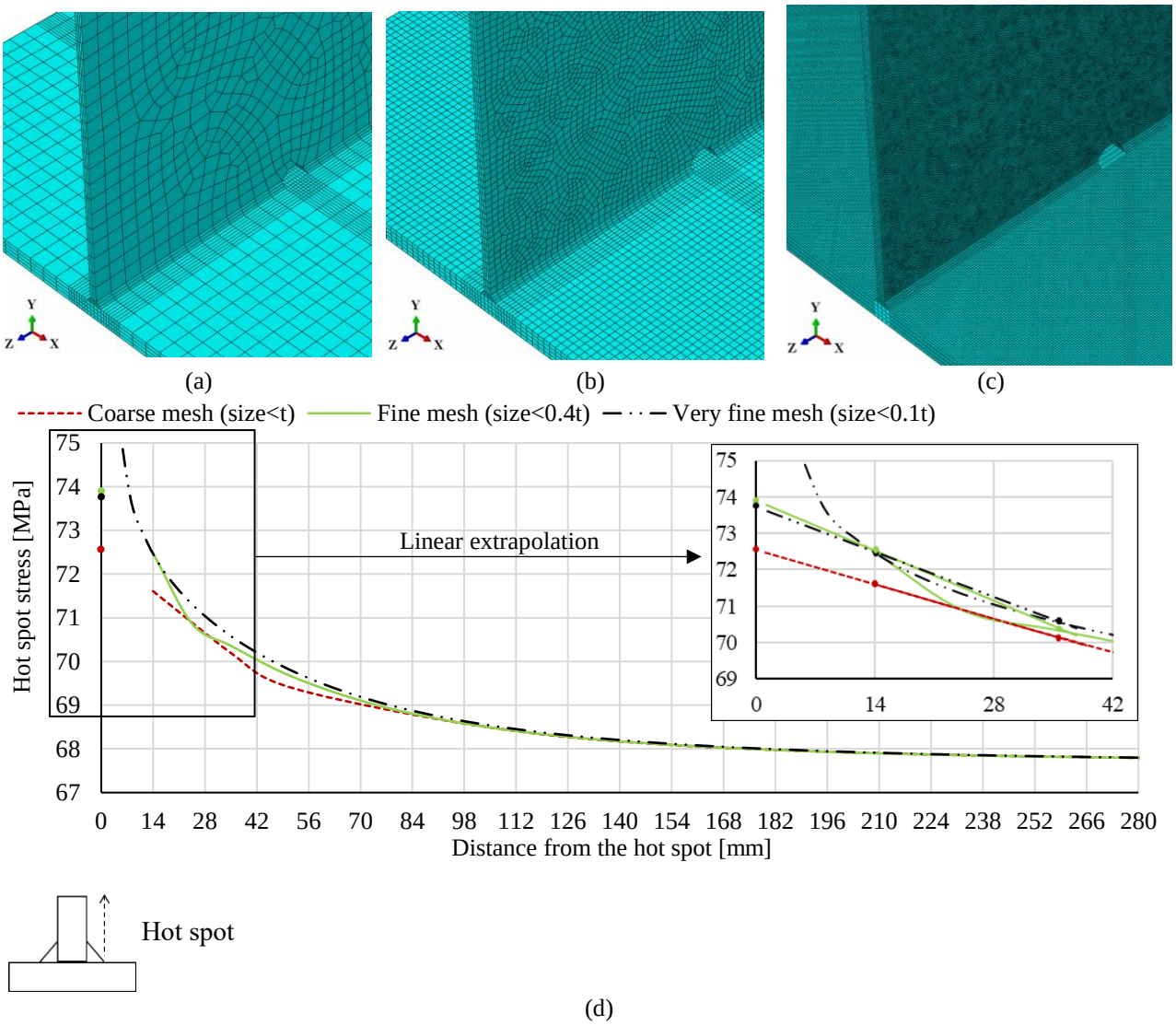


**Fig. 11.** Sensitivity analysis on mesh size for the HS at cope hole in transversal direction (HS1 in Fig 12b): (a) coarse mesh – size ≤ t, (b) fine mesh – size ≤ 0.4t, (c) very fine mesh – size ≤ 0.1t, (d) variation of the HS stress.

Based on the overview of sensitivity analysis in Table 4, which evaluates the maximum variation of computed HS stress between two subsequent sensitivity analysis steps, the optimal FE parameters were chosen resulting in a reasonable trade-off between convergence and analysis time. In sum, fine meshes were used for the rest of the fatigue design with element size not exceeding 0.4t, flanges/base plates are modelled with structured meshing and web is modelled with sweep meshing using the advancing front algorithm providing mapped meshes if appropriate (more details in Table 4), 8-noded linear solid elements with reduced integration were used (mesh refinement in thickness direction is applied with at least 4 elements), 1 m is used as L shown in Fig. 10 reproducing the BCs of the actual structural detail with no influence from another neighbouring critical detail (ensuring a homogenous stress field), linear extrapolation is used for the rest of the analysis as no sudden nonlinear changes in the loading direction is seen; fillet welds are modelled with an angle of 45° without convexity.

The cope holes are present in girders, mostly at the locations of butt welds on the flanges. Therefore, one of the sensitivity analyses relates to the presence of butt welds next to the cope hole. Guidance for the FE modelling of fillet welds may be found in the IIW guidelines. However, no further details are provided for the modelling of butt welds (such as on the curvature for example). In this research, the influence of the butt weld was studied by introducing its geometry in the cope hole with a radius of curvature of 13.75 mm. 6.90% variation in the HS stress, as described in Table 4, was noticed. As a result, the butt welds were not modelled together with cope holes but modelled as a separate (detail (h) in Fig. 6).

**Table 4.** Summary of sensitivity analyses.

| Sensitivity analysis | Maximum variation between computed HS stress [%] | Number of nodes [Max/Min] |
|---|---|---|
| Mesh size (varying between 0.1t and 1.0t) | 0.41 | 66.98 |
| Mesh topology [a] | 0.34 | 1.12 |
| Element type (8-node linear vs. 20-node quadratic) | 6.37 | 3.78 |
| Integration method (full vs. reduced integration) | 5.87 | - |
| Detail length (L in Fig. 10 varying between 0.5 m and 2 m) | 0.26 | 3.57 |
| Extrapolation method (linear vs. quadratic extrapolation) | 7.19 | - |
| Actual modelling of the butt weld | 6.90 | 1.04 |
| Shell vs. solid | 14.88 | 4.98 |
| Weld angle (varying between 30° and 60°) | 4.20 | 1.13 |
| Weld convexity (45° vs. convex and concave welds) | 3.34 | 1.05 |

[a] Because of geometrical discontinuity around the cope hole, webs are modelled with different meshing techniques (structured meshing vs. sweep meshing and medial axis algorithm vs. advancing front algorithm).

The HS stress can be calculated based on two extrapolation paths if applicable: in the transversal direction (HS1) and in the longitudinal one (HS2), as shown in Fig. 12(b). And stress extrapolation is performed via either linear or quadratic extrapolation function as shown in equations (7)-(8). The nonlinear extrapolation should be preferred over linear extrapolation if nonlinear structural stress increase is present at the vicinity of the weld bead with various gradients (Aygül et al., 2012; van Wingerde et al., 1995).

The fatigue lives are computed according to equations (9)-(10) considering the reference details available in (EN 1993-1-9, 2005; Hobbacher, 2016) for the HSSM.

Linear extrapolation : $\sigma_{HS} = 1.67\ \sigma_{0.4t} - 0.67\ \sigma_{1.0t}$ (7)

Quadratic extrapolation : $\sigma_{HS} = 2.52\ \sigma_{0.4t} - 2.24\ \sigma_{0.9t} + 0.72\ \sigma_{1.4t}$ (8)

For $10000 \leq 5\ 10^6$: $N = (\frac{\Delta\sigma_{FAT}}{\sigma_{HS}})^m . 2\ 10^6\ with\ m = 3$ (9)

For $5\ 10^6 \leq N$: $N = (\frac{\Delta\sigma_D}{\sigma_{HS}})^m . 5\ 10^6\ with\ m = 5$ (10)

where $t$ is the plate thickness, $\sigma_{HS}$ is the computed HS stress based on extrapolated stresses at 0.4t ($\sigma_{0.4t}$), 0.9t ($\sigma_{0.9t}$), 1.0t ($\sigma_{1.0t}$), or 1.4t ($\sigma_{1.4t}$), $N$ is the fatigue endurance of the evaluated detail, $\Delta\sigma_{FAT}$ is the reference detail provided in the IIW guideline which is FAT100 for transverse weld attachments, $\Delta\sigma_D$ is the stress at the constant amplitude fatigue limit (CAFL) for the same reference detail which is 73.68 MPa (m = 3) and m is the slope of the S-N curve

### 3.3.2 Fatigue life of the bridge details

The fatigue strength of the aforementioned critical details was assessed calculating the fatigue life with respect to HS stress range. Verification of the details is done by comparing the calculated fatigue endurance to $2\ 10^6$ cycles which corresponds to the detail category $\Delta\sigma_c$ according to (EN 1993-1-9, 2005). This comparison for the previously mentioned 3 most critical details can be seen in Fig. 12 for the design option made of EN 1.4162 under the stress state which corresponds to the equivalent stress range $\gamma_{Ff} . \gamma_{Mf} . \Delta\sigma_{E2}$. A summary of the results for each of the design options can be found in Table **5**. It can be seen that the fatigue resistance of each of detail is also verified according to HSSM for each design option.

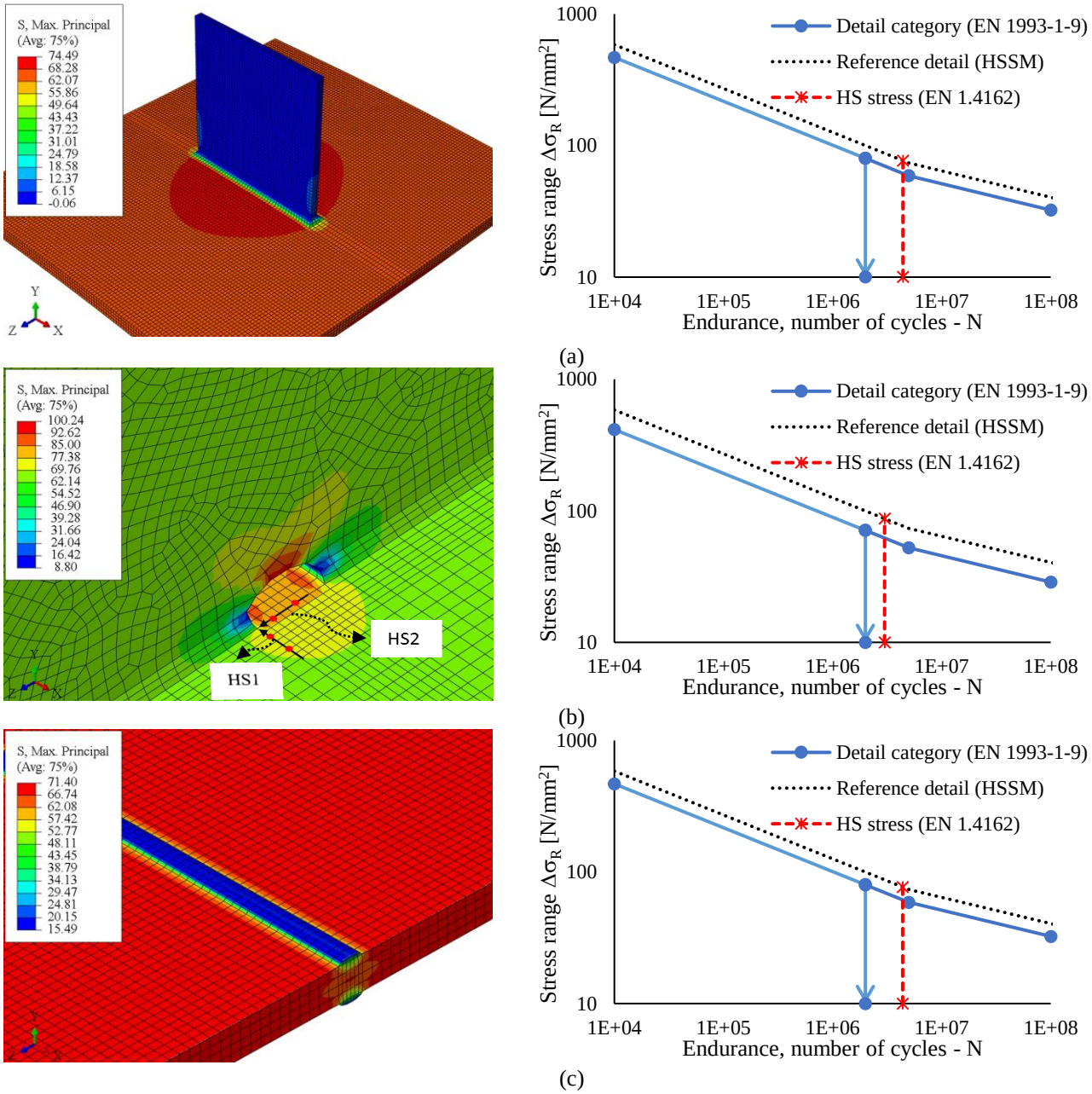


**Fig. 12.** Fatigue assessment following HSSM via FEM: (a) fatigue endurance of the transversal stiffener; (b) fatigue endurance of the cope hole; (c) fatigue endurance of the butt welds.

**Table 5.** Fatigue design of selected details according to HSSM.

| Detail | HS stress | | | Comparison with 2 $10^6$ [2 $10^6$ / N] – log scale | | |
|---|---|---|---|---|---|---|
| | S355 | EN 1.4162 | S460 | S355 | EN 1.4162 | S460 |
| (d) | 54.77 | 76.77 | 77.46 | 0.86 | 0.95 | 0.95 |
| (g) | 56.92 | 87.37 | 88.15 | 0.87 | 0.97 | 0.97 |
| (h)[a] | 54.88 | 76.91 | 77.60 | 0.86 | 0.95 | 0.95 |

[a] Size effect is considered

## 4 FINAL DESIGN RESULTS AND LIFECYCLE COST ASSESSMENT

### 4.1 Overview of design results

Table 6 gives an overview of the considered limit states and applied load-to-resistance ratios for each design option. Fatigue is the governing design criterion for the EN 1.4162 and S460 design options when either nominal stress method or HSSM is considered.

**Table 6.** Overview of each design result.

| Limiting design ratios | Controlling equation | S355 | EN 1.4162 | S460 |
|---|---|---|---|---|
| ULS – Positive flexure | $M_{Ed} / M_{c,Rd} \leq 1$ | 0.73 | 0.74 | 0.73 |
| ULS – Negative flexure | $M_{Ed} / M_{c,Rd} \leq 1$ | 0.89 | 0.93 | 0.92 |
| ULS -Shear | $V_{Ed} / V_{bw,Rd} \leq 1$ | 0.90 | 0.90 | 0.85 |
| ULS- Positive flexure and shear interaction | $M_{Ed} / M_{c,Rd} \leq 1$ | 0.73 | 0.75 | 0.73 |
| Is there interaction? | - | No | Yes | No |
| ULS- Negative flexure and shear interaction | $M_{Ed} / M_{c,Rd} \leq 1$ | 0.89 | 0.94 | 0.92 |
| Is there interaction? | - | No | Yes | No |
| FLS – NSM | $\gamma_{Ff} . \gamma_{Mf} . \Delta\sigma_{E2} / \Delta\sigma_c$ | 0.69 | 0.95 | 0.96 |
| FLS – HSSM | [2 $10^6$/N] – log scale | 0.87 | 0.97 | 0.97 |
| Controlling critical detail[a] | - | Detail (g) | Detail (g) | Detail (g) |
| SLS | $\delta(\psi_1 Q_{k1}) / (L/500)$ | 0.40 | 0.52 | 0.50 |

[a] In case the upgrade of the fatigue resistance of the detail categories for butt welds and cope holes is considered, detail (d) (transversal stiffeners) becomes the most critical detail for each design option.

### 4.2 Weight reduction

Table 7 provides an overview of the weight reduction resulting from the use of EN 1.4162 and S460 as compared to S355. The comparison is performed considering the main longitudinal girders of the bridge along the span CD in Fig. 2 with a variable cross-section distribution along the beam, the stiffeners and the cross beams. The same table also mentions the surface in need of corrosion protection which excludes the top surface of the girder top flange.

**Table 7.** Weight reduction and surface areas to be painted.

| Design comparison | Total weight | Reduction vs. S355 | Total surface | Coating requirement? | Surface area to be coated |
|---|---|---|---|---|---|
| | [Ton] | [%] | [$m^2$] | - | [$m^2$] |
| S355 | 435.70 | – | 2876.62 | Yes | 2652.15 |
| EN 1.4162 | 352.54 | 19.09 | 2934.84 | No | 2726.05 |
| S460 | 365.23 | 16.17 | 2949.06 | Yes | 2740.26 |

One can see that the use of EN 1.4162 and S460 leads to a quite significant weight reduction of the bridge superstructure, when compared to the design option using S355. It is important to note that the beneficial influence of strain hardening for stainless steel that could be taken into account through the use of the Continuous Strength Method (CSM) is not considered in the current study (Afshan and Gardner, 2013) even though it is today implemented in (DMSSS, 2017). Taking this effect into account would lead to an even lighter superstructure.

### 4.3 Comparison of initial costs

The initial costs of all design options were calculated according to (Rossi et al., 2017). While evaluating the carbon steel design options, the cost of initial painting was evaluated including the labour costs. The painting cost makes up about 30% of the material costs for the superstructure. In case high strength steel is used, it results in a small reduction of the initial painting costs of about 5%.

### 4.4 Comparison of total net present value at the life horizon of the bridge

While calculating the cost of maintenance, only the surfaces prone to corrosion are considered (i.e. the surfaces that are naturally protected against corrosion are disregarded such as the top surface of the top flanges). The corrosion intensity and treated surface dimensions are influential factors on the maintenance costs. According to (Rossi et al., 2017), 3 maintenance activities corresponding to three states can be considered: “Patch-Up” usually on 5% of the bridge surface after 12.8 years; “Overcoating” occurring after 18.5 years and “Remove and Replace” occurring after 31 years, both of the latter are assumed to be done over the surface exposed to corrosion. For more detailed information, the reader can refer to Chapter 3.3 of (Rossi et al., 2017) where average costs and time of occurrence for maintenance activities are given as well as their scatter. The selected years for the moment at which repair occurs are not gross approximations. They were based on a literature survey and on interviews with experts as described in (Rossi et al., 2017). It is not the purpose of the present analysis to repeat what has been done in (Rossi et al., 2017) but to apply the same analysis to the studied bridge.

The lifecycle cost assessment (LCCA) takes into account the changing value of money throughout the design lifespan making use of the net present value (NPV) and the net future value (NFV). The NFV predicts how profitable a design option is at the end of the design lifespan in comparison with a possible investment elsewhere. LCCA herein uses the predicted escalation rate ($i$) and discount rate ($d$). The discount rate makes a correlation between the NPV and NFV as it ensures that the discounted value of the NFV corresponds to the value at the present (considering the design lifespan of the bridge). The NFV and NPV for the occurring events in $n$ year(s) can be calculated using Equations(11)-(12):

Net Future Value: $NFV = C(1+i)^n$ (11)

Net Present Value: $NPV = C(\frac{1+i}{1+d})^n$ (12)

where $C$ is the present cost, $i$ is the escalation rate, $d$ is the discount rate and $n$ is the occurrence year of the cost (considering the previously mentioned maintenance activities). Presently the model sequence as defined in (Rossi et al., 2017) is considered. The NPV is calculated based on an escalation rate of 2 % and a discount rate of 5 %.

The ratios of assumed initial costs of the different design options compared to S355 are given in Table 8, resulting in the same total lifecycle cost (total NPV) at the life horizon of 75 years. It can be seen that if the initial cost of stainless steel EN 1.4162 is not 3.29 times higher than the cost of mild steel S355, the total NPV of both options are the same. Similarly, if the initial cost of high strength steel S460 is not 1.13 times higher than the cost of mild steel S355, their total lifecycle cost is the same. The schematic comparison of lifecycle costs of each design option can also be seen in Fig. 13.

**Table 8.** Ratio of initial costs of design options EN 1.4162 and S460 to that of S355.

| Design comparison | EN 1.4162 / S355 | S460 / S355 |
|---|---|---|
| Ratio of initial costs | 3.29 | 1.13 |

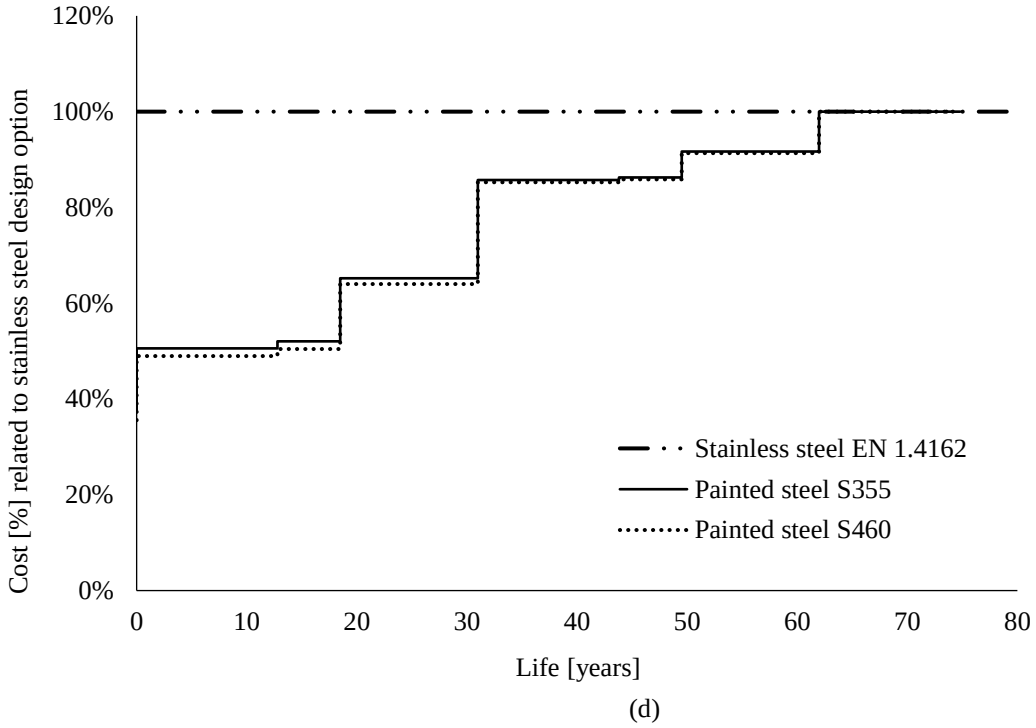


(d)

**Fig. 13.** Cost related to stainless steel design option.

## 5 CONCLUSIONS AND FUTURE WORKS

This paper investigates the advantages of using higher strength (carbon or stainless) steel members instead of S355 carbon steel in a welded girder bridge, benefiting both from weight reduction and maintenance costs. The higher strength steels considered in this study are the duplex stainless steel EN 1.4162 and the structural carbon steel grade S460. The initial designs of the bridge made of carbon steel S355 was performed by the civil structures design office "GRID International" as published in (Habraken et al., 2019; Lemma et al., 2020; Pedro et al., 2018, 2017). In the present study, the bridge was re-designed considering duplex stainless EN 1.4162 and S460 steel and it leads to a significant weight reduction thanks to higher yield strength and better fatigue resistance. The following conclusions can be drawn:

- A selection of welded fatigue prone details, which are typically seen in highway girder bridges, was done in accordance with a literature review. Each of them was verified globally using the nominal stress method under the application of the fatigue load model 3, and also locally using the hot spot stress method. Among each of the selected fatigue prone details, transversal stiffeners, full penetration butt welds of the flanges and cope holes turned out to be the most critical ones. It is noteworthy to mention that both the butt welds and cope holes have upgradable fatigue classes by simply modifying the weld convexity or bringing the welds to ground flush state. However, this statement does not apply to transversal stiffeners.

- In terms of weight reduction with respect to the design option S355, the designs made of EN 1.4162 and S460 have a weight gain of 19 % and 16 % respectively. While assessing the lifecycle cost, maintenance and material consumption should both be considered, where the maintenance herein mostly consists of activities done on the protective coatings (such as patching-up the damaged coating). In this case, moving from mild carbon steel S355 to high strength S460 only provides 3.2 % of reduction of the surface to be painted, which is also taken into account in the lifecycle cost. When the stainless steel option is studied, the surface needing maintenance is set to zero, which is in agreement with the Corrosion Resistance Class (CRC) and duplex grade.
- At the bridge life horizon (75 years), the LCCA shows that the total net present value of the cost of the S355 and the EN 1.4162 design options are equal if the initial price of stainless steel does not exceed 3.29 times the one of mild carbon steel, whereas the total NPV of S355 and S460 are equal if the initial cost of the higher strength steel option does not exceed 1.13 times the one of mild carbon steel. Note that this includes coating costs, which take into account labour costs as well. It is very interesting to notice that 3.29 is a reasonable multiplying factor which makes the stainless steel EN 1.4162 design option a realistic one. The same cannot be concluded for the design option S460. This therefore leads us to conclude that hybrid solutions made of EN 1.4162 and S460 combining corrosion resistance of stainless steel to lower initial cost of S460 would lead to even lower lifecycle cost.

### 6 ACKNOWLEDGEMENTS

The first author is funded by the Impulsfonds for the PhD project “3E160992” at KU Leuven.

## REFERENCES

Afshan, S., Gardner, L., 2013. The continuous strength method for structural stainless steel design. Thin-Walled Struct. 68, 42–49. https://doi.org/10.1016/j.tws.2013.02.011

Al-Emrani, M., Kliger, R., 2009. Fatigue prone details in steel bridges. Nordic Steel Construction Conference 2009, Malmö, Sweden, pp. 112–119.

ASCE, 1982. Fatigue Reliability: Introduction. J. Struct. Div. 108, 3–23.

Aygül, M., Al-Emrani, M., Urushadze, S., 2012. Modelling and fatigue life assessment of orthotropic bridge deck details using FEM. Int. J. Fatigue 40, 129–142. https://doi.org/10.1016/j.ijfatigue.2011.12.015

Baddoo, N.R., 2008. Stainless steel in construction: A review of research, applications, challenges and opportunities. J. Constr. Steel Res. 64, 1199–1206. https://doi.org/10.1016/j.jcsr.2008.07.011

Branco, C.M., Maddox, S.J., Sonsino, C.M., 2001. Fatigue design of welded stainless steels. European Commission.

Brozzetti, J., Hirt, M.A., Ryan, I., Sedlacek, G., Smith, I.F.C., 2018. Background Information on Fatigue Design Rules Statistical Evaluation. The European Convention for Constructional Steelwork (ECCS).

Budano, S., Kuppers, M., Kaufmann, H., Meisozo, A.M., Davis, C., 2007. Application of high strength steel plates to welded

deck components for ships and bridges subjected to medium/high service loads. European Commission.

Det Norske Veritas AS, 2011. DNV-RPC203, Fatigue Design of Offshore Steel Structures.

Doerk, O., Fricke, W., Weissenborn, C., 2003. Comparison of different calculation methods for structural stresses at welded joints. Int. J. Fatigue 25, 359–369. https://doi.org/10.1016/S0142-1123(02)00167-6

Duga, J.J., Fisher, W.H., Buxbaum, R.W., Rosenfield, A.R., Buhr, A.R., Honton, E.J., McMillan, S.C., 1983. The Economic Effects of Fracture in the United States Part 2 — A Report to NBS by Battelle Columbus Laboratories, National Bureau of Standards Special Publication. National Bureau of Standards.

European Committee for Standardization, 2019. EN 10025-3, Hot rolled products of structural steels - Part 3: Technical delivery conditions for normalized/normalized rolled weldable fine grain structural steels. CEN, Brussels.

European Committee for Standardization, 2014. EN 10088-2, Stainless steels - Part 2: Technical delivery conditions for sheet/plate and strip of corrosion resisting steels for general purposes. CEN, Brussels. https://doi.org/10.1007/BF00655030

European Committee for Standardization, 2002. EN 1990, Eurocode 0 - Basis of structural design. CEN, Brussels.

European Committee for Standardization, 2012. EN 1990 ANB, Eurocode 0 - Basis of structural design - National annex. CEN, Brussels.

European Committee for Standardization, 2005. EN 1991-1-4, Eurocode 1: Actions on structures - Part 1-4: General actions - Wind actions. CEN, Brussels.

European Committee for Standardization, 2010. EN 1991-1-4 ANB, Eurocode 1 : Actions on structures - Part 1-4 : General actions - Wind actions - National annex. CEN, Brussels.

European Committee for Standardization, 2003. EN 1991-2, Eurocode 1: Actions on structures - Part 2: Traffic loads on bridges. CEN, Brussels.

European Committee for Standardization, 2011. EN 1991-2 ANB, Eurocode 1 : Actions on structures - Part 2 : Traffic loads on bridges - National annex. CEN, Brussels.

European Committee for Standardization, 2005. EN 1993-1-1, Eurocode 3: Design of steel structures - Part 1-1: General rules and rules for buildings. CEN, Brussels.

European Committee for Standardization, 2005. EN 1993-1-10, Eurocode 3: Design of steel structures - Part 1-10: Material toughness and through-thickness properties. CEN, Brussels.

European Committee for Standardization, 2006. EN 1993-1-4, Eurocode 3 - Design of steel structures - Part 1-4: General rules - Supplementary rules for stainless steels. CEN, Brussels.

European Committee for Standardization, 2015. EN 1993-1-4, Eurocode 3 - Design of steel structures - Part 1-4: General rules - Supplementary rules for stainless steels. CEN, Brussels.

European Committee for Standardization, 2006. EN 1993-1-5, Eurocode 3 - Design of steel structures - Part 1-5: Plated structural elements. CEN, Brussels.

European Committee for Standardization, 2005. EN 1993-1-8, Eurocode 3: Design of steel structures - Part 1-8: Design of joints. CEN, Brussels.

European Committee for Standardization, 2005. EN 1993-1-9, Eurocode 3: Design of steel structures - Part 1-9: Fatigue. CEN, Brussels.

European Committee for Standardization, 2006. EN 1993-2, Eurocode 3 - Design of steel structures - Part 2: Steel Bridges. CEN, Brussels.

European Committee for Standardization, 2004. EN 1994-1-1, Eurocode 4: Design of composite steel and concrete structures

- Part 1-1: General rules and rules for buildings. CEN, Brussels.

European Committee for Standardization, 2005. EN 1994-2, Eurocode 4 - Design of composite steen and concrete structures - Part 2: General rules and rules for bridges. CEN, Brussels.

Euro Inox/SCI, 2017. Design manual for structural stainless steel., 4th ed. Euro Inox and the Steel Construction Institute.

Ericsson, C., Johansson, P., Liljas, M., Westin, E.M., 2003. MECHANICAL PROPERTIES OF WELDS IN THE NEW LEAN DUPLEX STAINLESS STEEL LDX 2101® (EN 1.4162, UNS S32101), in: Stainless Steel World. The Hague.

Fortan, M., Dejans, A., Karabulut, B., Debruyne, D., Rossi, B., 2020. On the strength of stainless steel fillet welds. J. Constr. Steel Res. 170. https://doi.org/10.1016/j.jcsr.2020.106081

Fricke, W., Cui, W., Kierkegaard, H., Kihl, D., Koval, M., Mikkola, T., Parmentier, G., Toyosada, M., Yoon, J.H., 2002. Comparative fatigue strength assessment of a structural detail in a containership using various approaches of classification societies. Mar. Struct. 15, 1–13. https://doi.org/10.1016/S0951-8339(01)00016-8

Fricke, W., Gao, L., Paetzold, H., 2017. Fatigue assessment of local stresses at fillet welds around plate corners. Int. J. Fatigue 101, 169–176. https://doi.org/10.1016/j.ijfatigue.2017.01.011

Günther, H., 2005. Use and application of high-performance steels for steel structures. IABSE-AIPC-IVBH.

Habraken, A.M., Duchêne, L., Bouffioux, C., Kuhlmann, U., Zizza, A., Breunig, S., Pourostad, V., Da Silva, L., Rebelo, C., Gervasio, H., Rigueiro, C., Maas, F., Baaten, T., Droesbeke, B., Reis, A., Pedro, J., Baptista, C., Virtuoso, F., Vieira, C., Dufrane, J.J., Vanderbecq, A.C., Toussaint, P., 2019. Optimal use of High Strength Steel grades within bridge (OPTIBRI). European Commission. https://doi.org/10.2777/93807

Haghani, R., Al-emrani, M., Heshmati, M., 2012. Fatigue-Prone Details in Steel Bridges 456–476. https://doi.org/10.3390/buildings2040456

Hobbacher, A.F., 2016. Recomendations for Fatigue Design of Welded Joints and Components, 2nd ed, IIW collection. International Institute of Welding (IIW), Springer International Publishing. https://doi.org/10.1007/978-3-319-23757-2

Iversen, A.K., 2006. Stainless steels in bipolar plates-Surface resistive properties of corrosion resistant steel grades during current loads. Corros. Sci. 48, 1036–1058. https://doi.org/10.1016/j.corsci.2005.05.012

Ji, B., Liu, R., Chen, C., Maeno, H., Chen, X., 2013. Evaluation on root-deck fatigue of orthotropic steel bridge deck. J. Constr. Steel Res. 90, 174–183. https://doi.org/10.1016/j.jcsr.2013.07.036

Karabulut, B., Lombaert, G., Debruyne, D., Rossi, B., 2020. Experimental and numerical fatigue assessment of duplex welded transversal stiffeners. Int. J. Fatigue 134. https://doi.org/10.1016/j.ijfatigue.2020.105498

Karabulut, B., Rossi, B., Lombaert, G., Debruyne, D., 2018. Optimized design and life cycle cost analysis of a duplex welded girder bridge, in: The 6th International Symposium on Life-Cycle Civil Engineering, IALCCE 2018. CRC Press, Ghent, pp. 2715–2722.

Kubiš, P., Ryjáček, P., 2017. Behaviour of several fatigue prone bridge details. IOP Conf. Ser. Mater. Sci. Eng. 236. https://doi.org/10.1088/1757-899X/236/1/012065

Lagerqvist, O., Clarin, M., Gozzi, J., Völling, B., Pak, D., Stötzi, J., Lieurade, H., Depale, B., Huther, I., Herion, S., Bergers, J., Martsch, R., Carlsson, M., Samuelsson, A., Sonander, C., 2007. Efficient lifting equipment with extra high-strength steel. European Commission, Research Fund for Coal and Steel (RFCS).

Lee, J.-M., Seo, J.-K., Kim, M.-H., Shin, S.-B., Han, M.-S., Park, J.-S., Mahendran, M., 2010. Comparison of hot spot stress evaluation methods for welded structures. Int. J. Nav. Archit. Ocean Eng. 2, 200–210. https://doi.org/10.2478/IJNAOE-2013-0037

Lemma, M.S., Gervásio, H., Pedro, J.O., Rigueiro, C., da Silva, L.S., 2020. Enhancement of the life-cycle performance of bridges using high-strength steel. Struct. Infrastruct. Eng. 16, 772–786.

https://doi.org/10.1080/15732479.2019.1662067

Liljas, M., Ericsson, C., 2002. Fatigue behaviour of stainless steel welds, in: AvestaPolarit Corrosion Management and Application Engineering.

Liu, R., Liu, Y., Ji, B., Wang, M., Tian, Y., 2014. Hot spot stress analysis on rib-deck welded joint in orthotropic steel decks. J. Constr. Steel Res. 97, 1–9. https://doi.org/10.1016/j.jcsr.2014.01.012

Lukic, M., Kühn, B., 2020. From Assessment to Best Practice A Collection of Historical Fatigue Damage Cases in Steel and Composite Bridges. ECCS – European Convention for Constructional Steelwork.

Merello, R., Botana, F.J., Botella, J., Matres, M.V., Marcos, M., 2003. Influence of chemical composition on the pitting corrosion resistance of non-standard low-Ni high-Mn–N duplex stainless steels. Corros. Sci. 45, 909–921. https://doi.org/10.1016/S0010-938X(02)00154-3

Morgan, M.R., Lee, M.M.K., 1997. New parametric equations for stress concentration factors in tubular K-joints under balanced axial loading. Int. J. Fatigue 19, 309–317. https://doi.org/10.1016/S0142-1123(96)00081-3

Niemi, E., Fricke, W., Maddox, S.J., 2018. Structural Hot-Spot Stress Approach to Fatigue Analysis of Welded Components, Fatigue Analysis of Welded Components: Designer's Guide to the Structural Hot-Spot Stress Approach, IIW Collection. Springer Singapore. https://doi.org/10.1007/978-981-10-5568-3

Niemi, E., Fricke, W., Maddox, S.J., 2006. Fatigue Analysis of Welded Components Designer's guide to the structural hot-spot stress approach (IIW-1430-00), International Institute of Welding. The International Institute of Welding (IIW). https://doi.org/10.1017/CBO9781107415324.004

Nussbaumer, A., Borges, L., Davaine L., 2011. Fatigue Design of Steel and Composite Structures, 1st ed. ECCS – European Convention for Constructional Steelwork.

Olsson, J., Snis, M., 2007. Duplex - A new generation of stainless steels for desalination plants. Desalination 205, 104–113. https://doi.org/10.1016/j.desal.2006.02.051

Park, J.Y., Kim, H.-K., 2014. Fatigue life assessment for a composite box girder bridge. Int. J. Steel Struct. 14, 843–853. https://doi.org/10.1007/s13296-014-1215-x

Pedro, J.J.O., Reis, A.J., Baptista, C., 2018. High Strength Steel S690 in highway bridges: General guidelines for design. Stahlbau 87, 555–564. https://doi.org/10.1002/stab.201810615

Pedro, J.J.O., Reis, A.J., Baptista, C., 2017. High strength steel (HSS) S690 in highway bridges: Comparative design, in: Eurosteel 2017. EUROSTEEL 2017, Ernst and Sohn A Wiley Brand, Copenhagen, pp. 4059–4068. https://doi.org/10.1002/cepa.462

Peng, Y., Chen, J., Dong, J., 2019. Experimental data assessment and fatigue design recommendation for stainless-steel welded joints. Metals (Basel). 9. https://doi.org/10.3390/met9070723

Poutiainen, I., Tanskanen, P., Marquis, G., 2004. Finite element methods for structural hot spot stress determination - A comparison of procedures. Int. J. Fatigue 26, 1147–1157. https://doi.org/10.1016/j.ijfatigue.2004.04.003

Reed, R.P., Smith, J.H., Christ, B.W., 1983. The economic effects of fracture in the United States Part 1 — A Synopsis of the September 30, 1982 Report to NBS by Battelle Columbus Laboratories, National Bureau of Standards Special Publication. National Bureau of Standards Special Publication.

Rossi, B., Marquart, S., Rossi, G., 2017. Comparative life cycle cost assessment of painted and hot-dip galvanized bridges. J. Environ. Manage. 197, 41–49. https://doi.org/10.1016/j.jenvman.2017.03.022

Sedlacek, G., Hoffmeister, B., Müller, C., Kühn, B., Puthli, R., Herion, S., Karcher, D., Fleischer, O., Hanswille, G., Schmitt, C., Schleich, J., Cajot, L., Galea, Y., Lequien, P., Hegger, J., Döinghaus, P., 2002. Use of high-strength steel S460. European Commission.

Shi, G., Hu, F., Shi, Y., 2014. Recent research advances of high strength steel structures and codification of design

specification in China. Int. J. Steel Struct. 14, 873–887. https://doi.org/10.1007/s13296-014-1218-7

van Wingerde, A.M., Packer, J.A., Wardenier, J., 1995. Criteria for the fatigue assessment of hollow structural section connections. J. Constr. Steel Res. 35, 71–115. https://doi.org/10.1016/0143-974X(94)00030-I

Wei, Z., Laizhu, J., Jincheng, H., Hongmei, S., 2008. Study of mechanical and corrosion properties of a Fe-21.4Cr-6Mn-1.5Ni-0.24N-0.6Mo duplex stainless steel. Mater. Sci. Eng. A 497, 501–504. https://doi.org/10.1016/j.msea.2008.07.062

Xiao, Z.G., Yamada, K., 2004. A method of determining geometric stress for fatigue strength evaluation of steel welded joints. Int. J. Fatigue 26, 1277–1293. https://doi.org/10.1016/j.ijfatigue.2004.05.001

Ye, X.W., Su, Y.H., Han, J.P., 2014. A state-of-the-art review on fatigue life assessment of steel bridges. Math. Probl. Eng. 2014. https://doi.org/10.1155/2014/956473

Zilli, G., Maiorana, E., Peultier, J., Fanica, A., Hechler, O., Rauert, T., Maquoi, R., 2008. Application of duplex stainless steel for welded bridge construction in an aggressive environment, European Commision. European Commission, Research Fund for Coal and Steel (RFCS).